Supporting Information

In-situ construction of α-MoC/g-C_3N_4 Mott-Schottky heterojunction for efficient photocatalytic H_2 evolution

Jianfei Du [a#], Yongli Shen [b#], Fan Yang [a*], Bo Zhang [a], Xinzhi Jiang [a], Changhua An [a, b$], Jinhua Ye [c, d, e]

[a] *Tianjin Key Laboratory of Organic Solar Cells and Photochemical Conversion, School of Chemistry and Chemical Engineering, Tianjin University of Technology, Tianjin 300384, P. R. China*

[b] *Tianjin Key Laboratory of Advanced Functional Porous Materials, Institute of New Energy Materials & Low-Carbon Technologies, School of Materials Science and Engineering, Tianjin University of Technology, Tianjin 300384, China*

[c] *TU-NIMS Joint Research Center, School of Materials Science and Engineering, Tianjin University, Tianjin 300072, PR China*

[d] *Photocatalytic materials group, International Center for Materials Nanoarchitectonics (WPI-MANA), National Institute for Materials Science, 1-1 Namiki, Tsukuba,Ibaraki 305-0044, Japan*

[e] *Graduate School of Chemical Science and Engineering, Hokkaido University, Sapporo 060-0814, Japan*

Jianfei Du[#] and Yongli Shen[#] contributed equally to this work.

* Corresponding Author. E-mail: fanyang@email.tjut.edu.cn

[$] Corresponding Author. E-mail: anchua@ustc.edu

Contents

Fig.S1. XRD patterns of 3atz, HAM, m-3atz/HAM, and Mo-3atz............................S-4

Fig.S2. FT-IR spectra of HAM, 3atz, and Mo-3atz...S-5

Fig.S3. SEM images of Mo-3atz S-6

Fig. S4. SEM images of Mo-3atz synthesized under 70 °C (a, b), and as-prepared α-MoC (c, d)..S-7

Fig. S5. XRD pattern of Mo-3atz calcined under Ar atmosphere S-8

Fig.S6. XRD patterns of Mo-3atz precursor calcined under various temperatures....S-9

Fig.S7. XRD patterns of samples synthesized using other ligands S-10

Fig.S8. N_2 adsorption-desorption isotherms of of CN and MC-15/CN...................S-11

Fig.S9. The high-resolution O 1s spectrum of of α-MoC..S-12

Fig.S10. XRD patterns of MC-15/CN photocatalyst before and after the recycle test S-13

Fig.S11. HRTEM image and (b) EDS element mapping of MC-15/CN photocatalyst after the recycle test S-14

Fig.S12. LSV (a) and Tafel (b) curves of CN, MC-15/CN and MC S-15

Fig.S13. The models of H* adsorption sites on the surface of g-C_3N_4: (a) C site, and (b) N site S-16

Fig.S14. The models of H* adsorption sites of on the surface of α-MoC (α-MoC/g-C_3N_4): (a) C_1 site, (b) Mo_1 site, (c) Mo_2 site, (d)Mo_3 site, and (e) Mo_4 site S-17

Table S1. Comparison of the synthesis temperature and size of molybdenum carbide from literatures...S-18

Table S2. Comparison of various cocatalysts coupled with g-C_3N_4 photocatalyst for solar H_2 evolution from literatures...S-19

Table S3. Kinetic analysis of emission decay of g-C_3N_4 and composite photocatalysts S-20

Table S4. The ΔG_{H*} values of all the adsorption models S-21

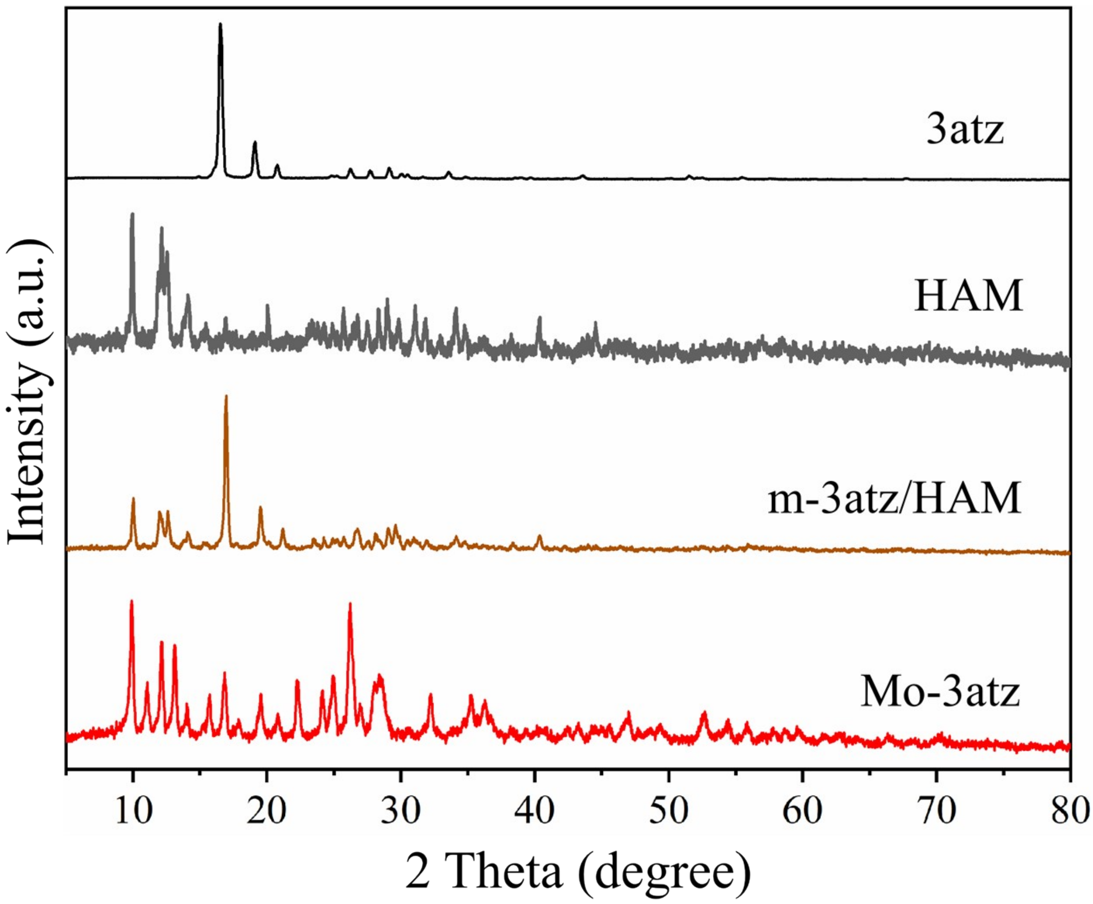

Fig. S1. XRD patterns of 3atz, HAM, m-3atz/HAM, and Mo-3atz.

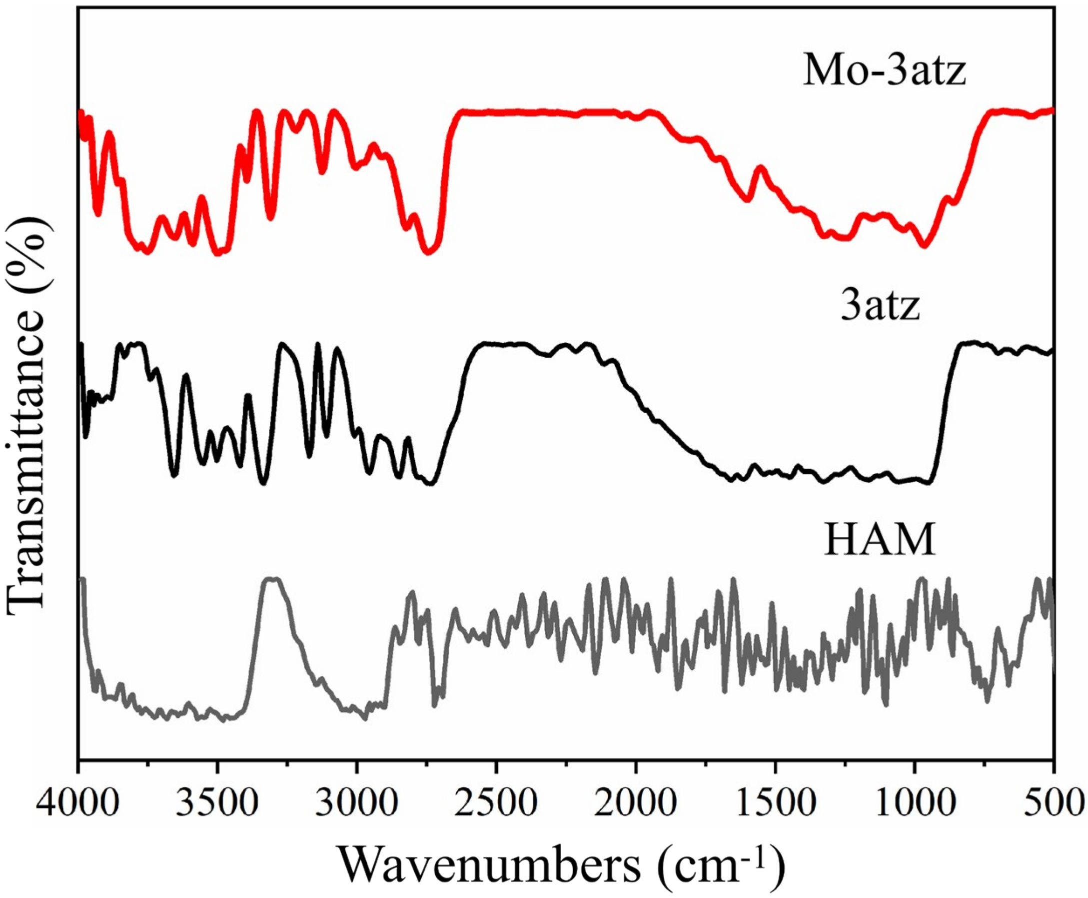

Fig. S2. FT-IR spectra of HAM, 3atz, and Mo-3atz.

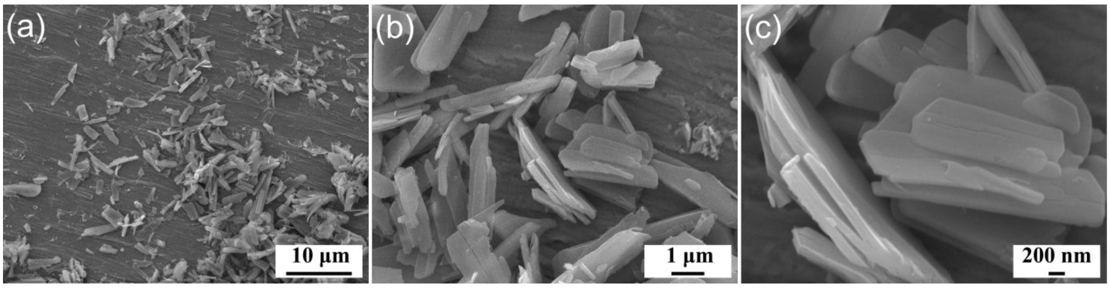

Fig. S3. SEM images of Mo-3atz synthesized in room temperature.

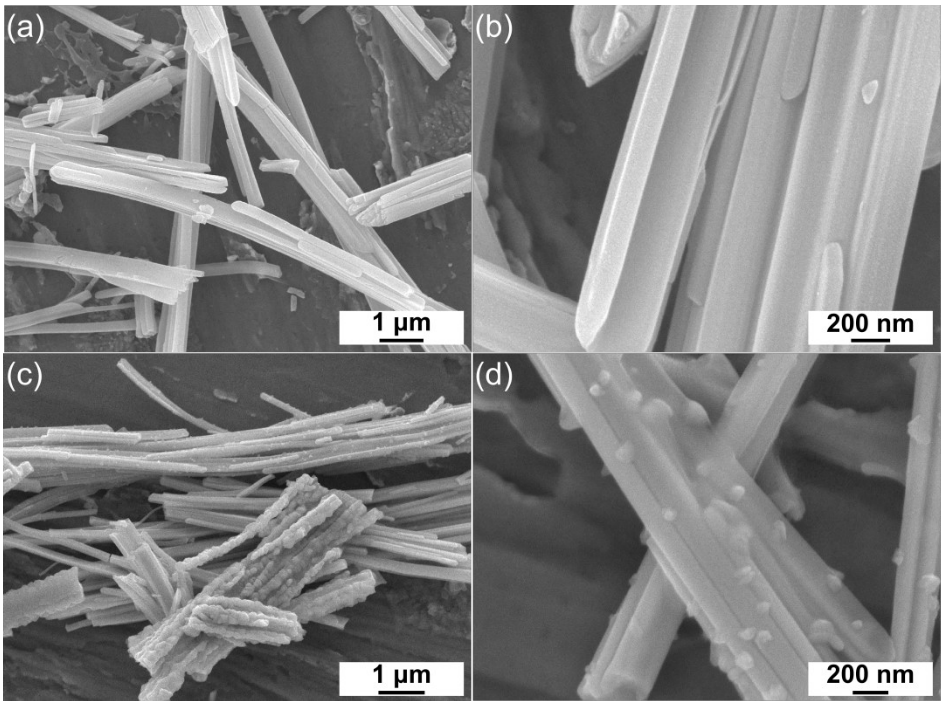

Fig. S4. SEM images of Mo-3atz synthesized under 70 °C (a, b), and as-prepared α-MoC (c, d)

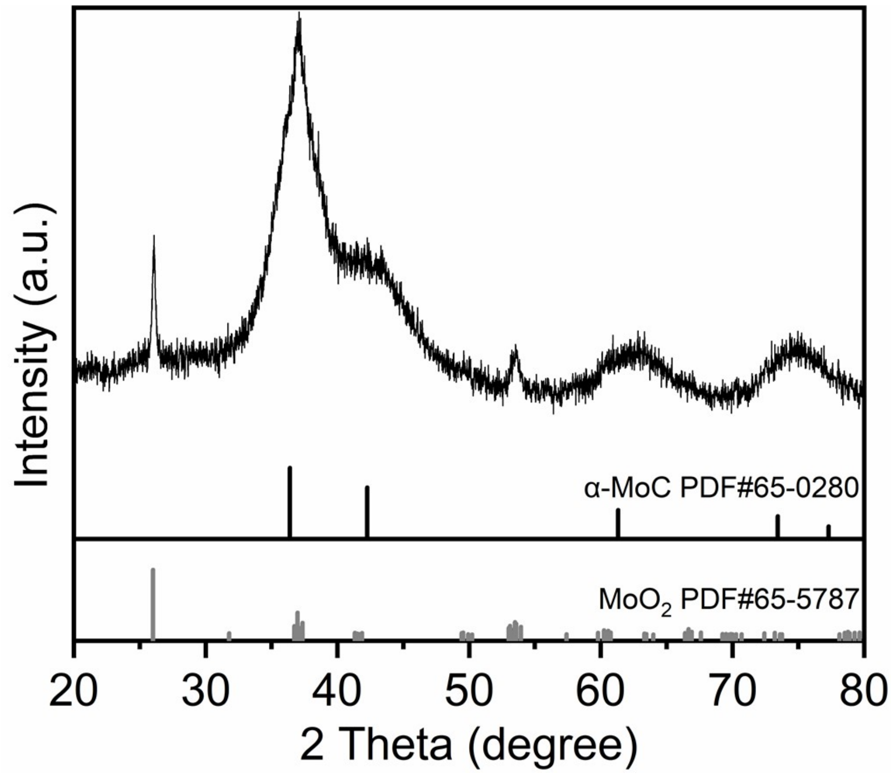

Fig. S5. XRD pattern of Mo-3atz calcined under Ar atmosphere.

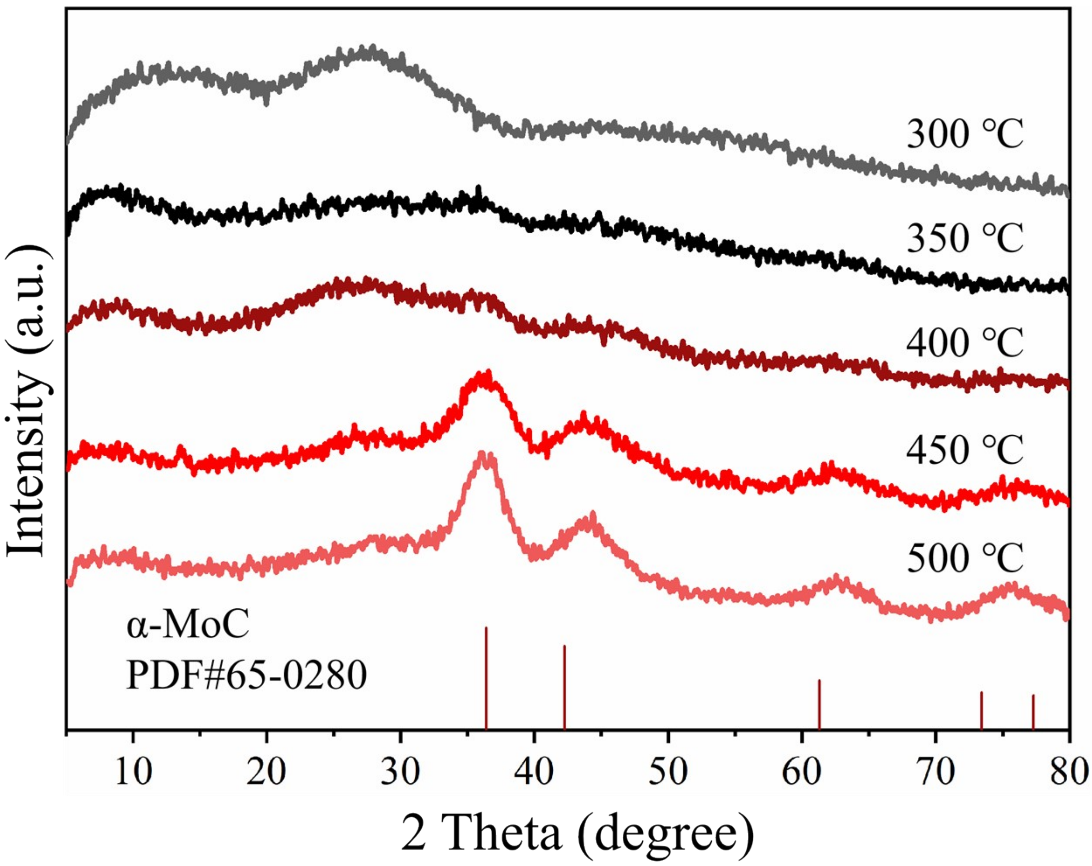

Fig. S6. XRD patterns of Mo-3atz precursor calcined under various temperatures.

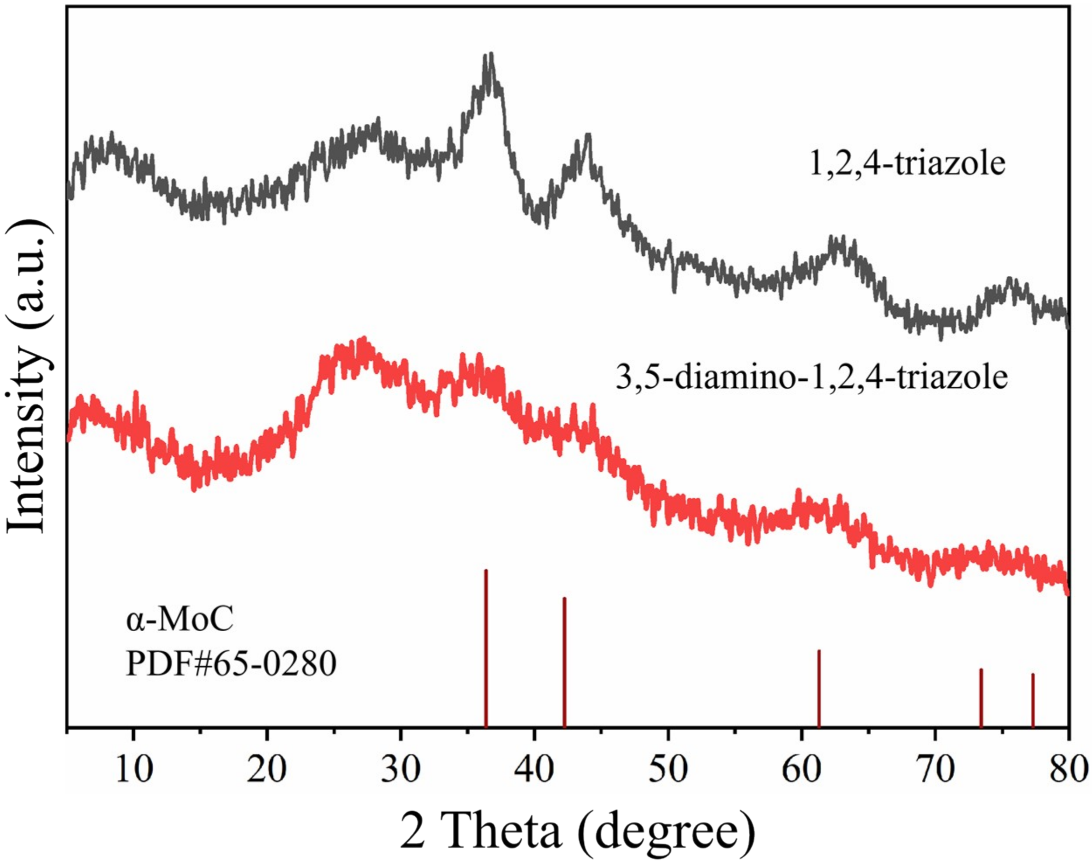

Fig. S7. XRD patterns of samples synthesized using other ligands.

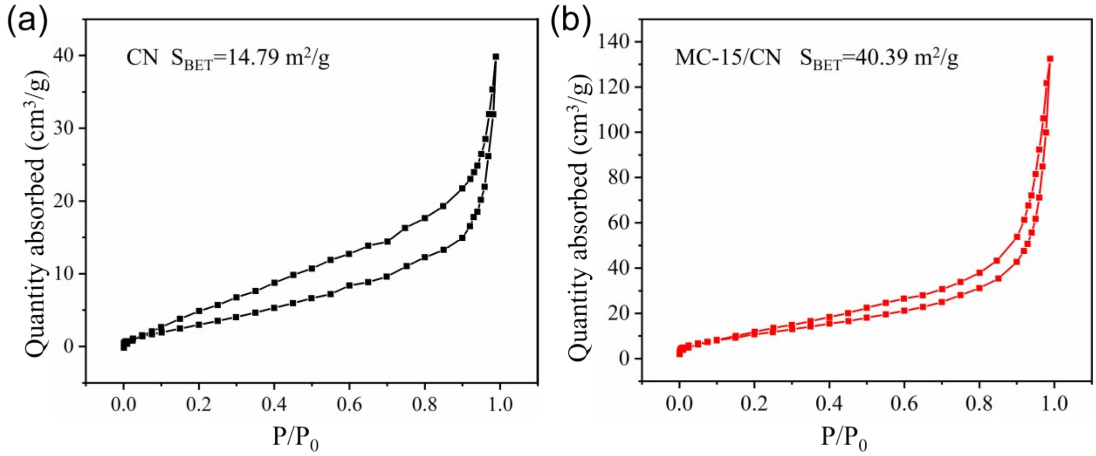

Fig. S8. N_2 adsorption-desorption isotherms of CN and MC-15/CN.

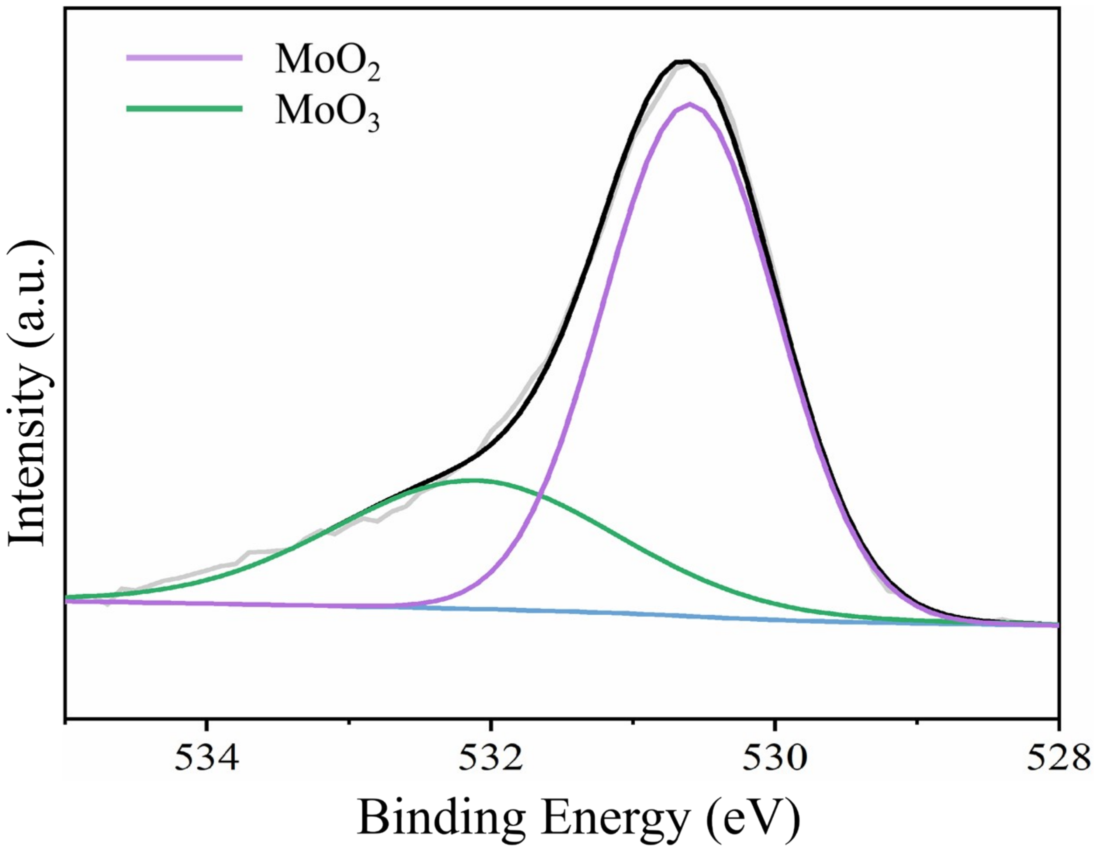

Fig. S9. The high-resolution O 1s spectrum of of α-MoC.

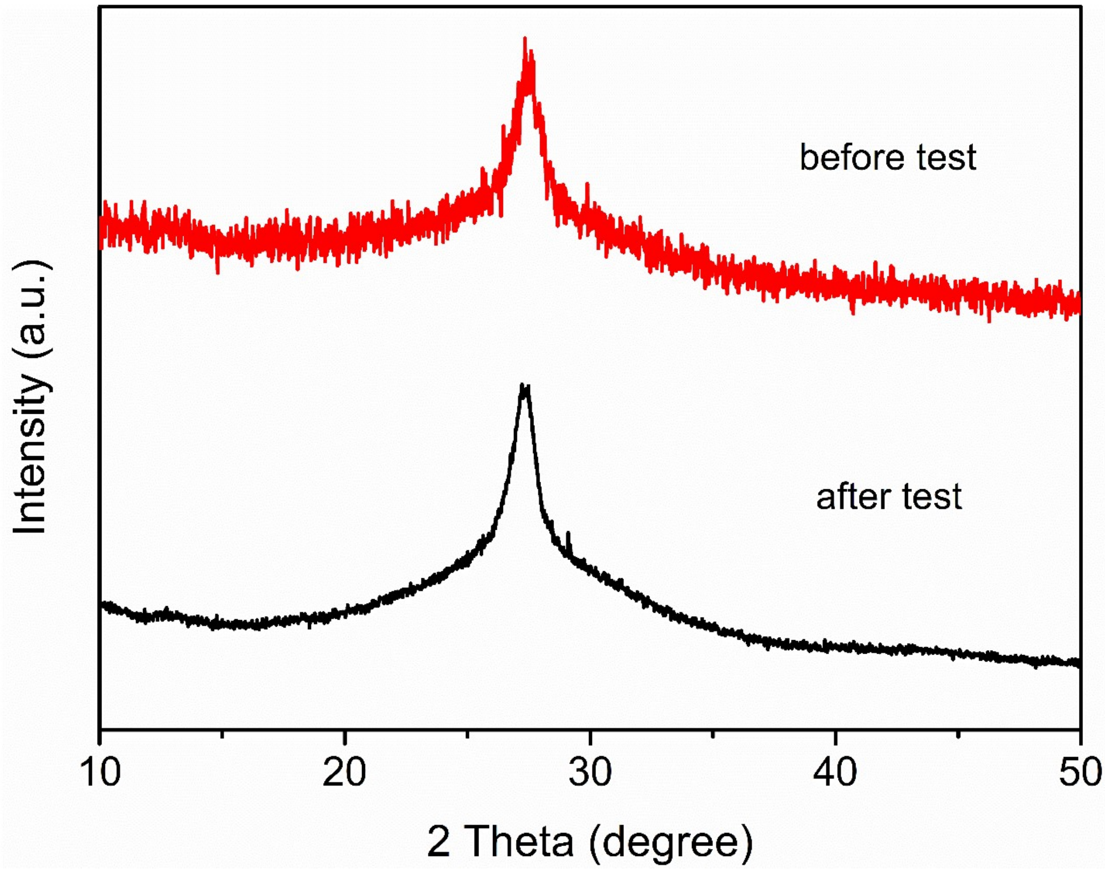

Fig. S10. XRD patterns of MC-15/CN photocatalyst before and after the recycle test.

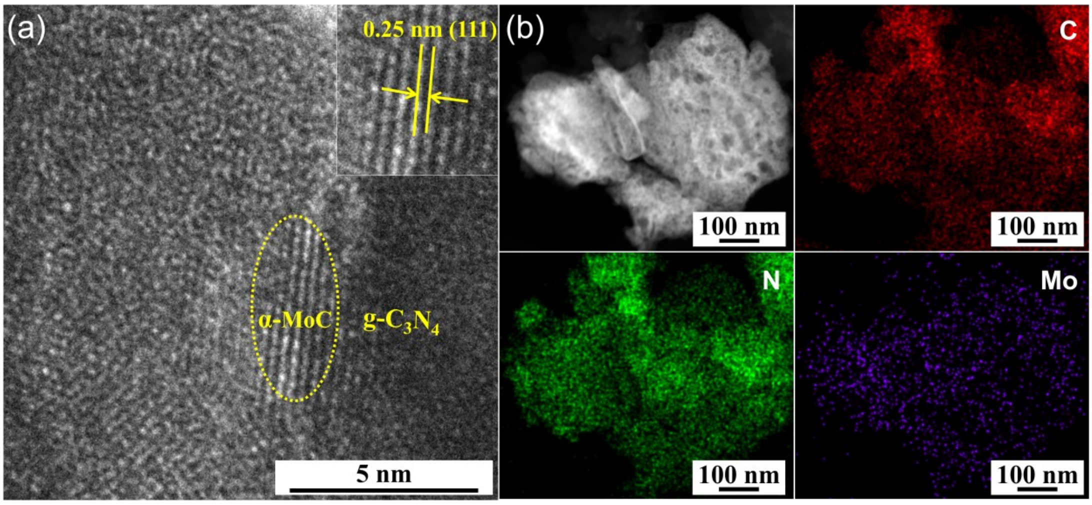

Fig. S11. (a) HRTEM image and (b) EDS element mapping of MC-15/CN photocatalyst after the recycle test.

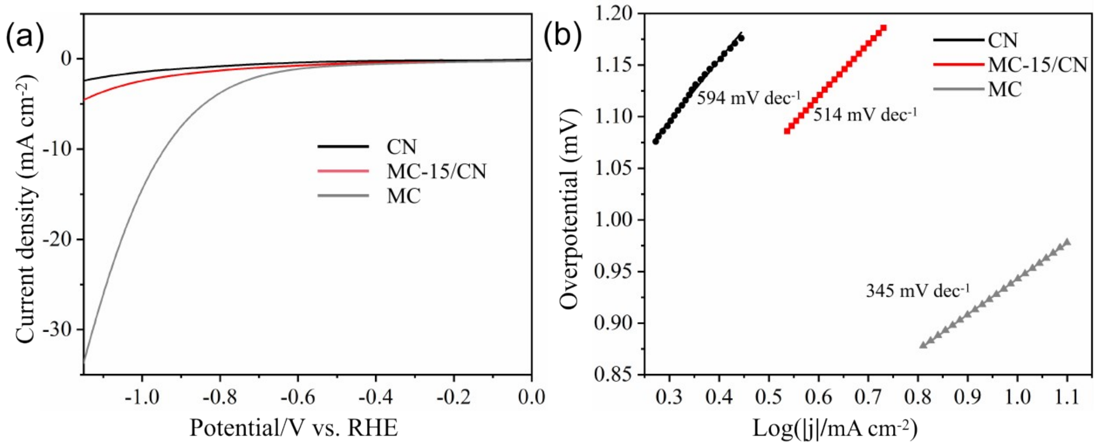

Fig. S12. LSV (a) and Tafel (b) curves of CN, MC-15/CN and MC.

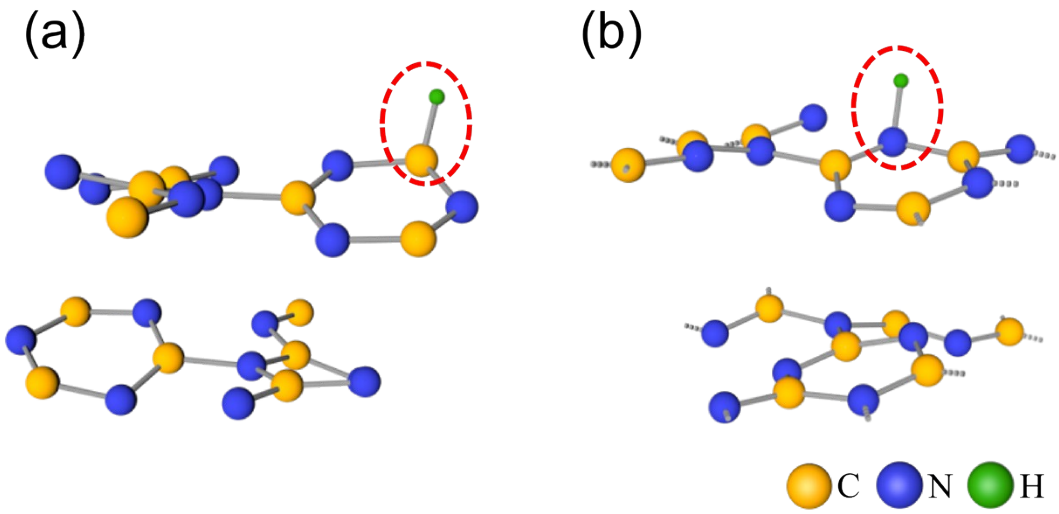

Fig. S13. The models of H* adsorption sites on the surface of g-C_3N_4: (a) C site, and (b) N site.

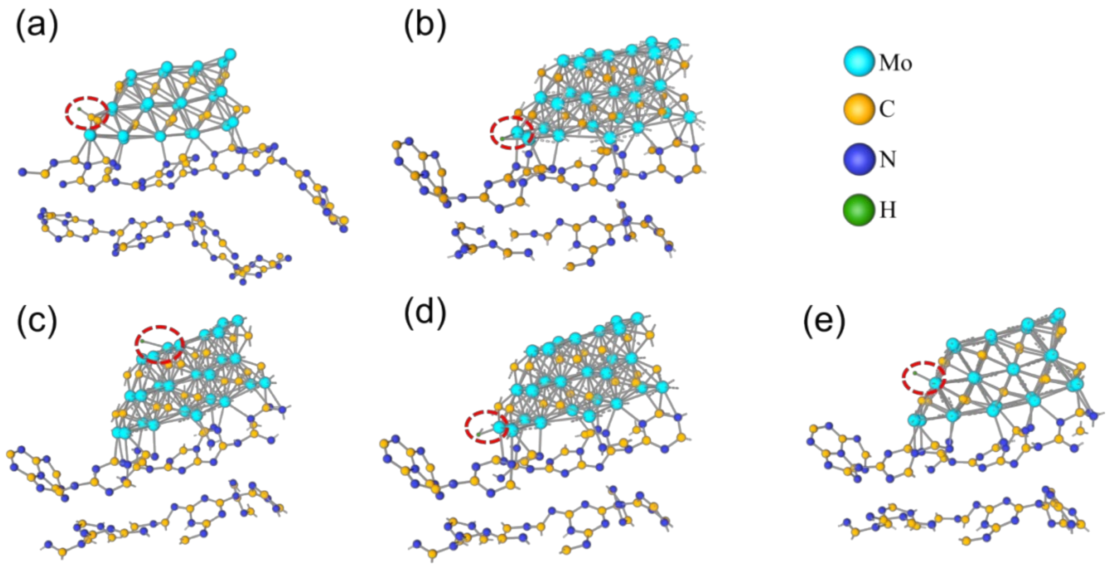

Fig. S14. The models of H* adsorption sites of on the surface of α-MoC (α-MoC/g-C_3N_4): (a) C_1 site, (b) Mo_1 site, (c) Mo_2 site, (d)Mo_3 site, and (e) Mo_4 site.

Table S1. Comparison of the synthesis temperature and size of molybdenum carbide from literatures.

Material	Synthesis temperature (°C)	Atmosphere	Size (nm)	Reference
MoC	1000	Ar	~5	1
Mo_xC	1000	Ar	8.9 ± 3.4	2
C-Mo_xC	900	N_2	1-3 (ball mill)	3
Mo_2C	800	Ar	14.9	4
Mo_2C	800	Ar	~8.5	5
MoC	800	NH_3	7	6
MoC	800	N_2	~5	7
Mo_2C@C	800	Inert	~5	8
Mo_2C	800	Ar	~4	9
Mo_2C	800	Ar	3-5	10
Mo_2C	750	Ar	~3	11
α-MoC	720	CH_4/H_2	~10	12
α-MoC	700	NH_3, CH_4/H_2	5-10	13
α-MoC	700	NH_3, CH_4/H_2	2-5	14
MoC-QDs/C	700	Ar	2-5	15
Mo_2C	675	Ar	6.8 ± 1.3	16
α-MoC	**450-550**	**H_2/Ar**	**~1.8**	**This work**

Table S2. Comparison of various cocatalysts coupled with g-C_3N_4 photocatalyst for solar H_2 evolution from literatures.

Photocatalyst	Sacrificial agent	Light source	H_2 evolution rate (μmol h^{-1} g^{-1})	Ref
Mo_2C/g-C_3N_4	TEOA	300 W Xe lamp (λ > 420 nm)	60.9	17
2.0wt.% Mo-Mo_2C/g-C_3N_4	TEOA	300 W Xe lamp (λ > 420 nm)	219	17
MoC-Li/g-C_3N_4	TEOA	300 W Xe lamp (λ > 420 nm)	130	9
CN-1M (Mo_2C/g-C_3N_4)	TEOA	300W Xe lamp (λ > 420 nm)	507	18
$MoSe_2$/g-C_3N_4	TEOA	300 W Xe lamp (λ > 420 nm)	136.8	19
WC/g-C_3N_4	TEOA	300 W Xe lamp (λ > 420 nm)	146.1	20
WS_2/g-C_3N_4	TEOA	300 W Xe lamp (1.5 W cm^{-2})	154	21
Ni_2P/g-C_3N_4	TEOA	300 W Xe lamp (λ > 420 nm)	82.5	22
2% MWNTS/g-C_3N_4	Methanol	300 W Xe lamp (λ > 400 nm)	75.8	23
MC-15/CN	**TEOA**	**300 W Xe lamp (λ > 400 nm)**	**180**	**This work**

Table S3. Kinetic analysis of emission decay of g-C_3N_4 and composite photocatalysts.

Samples	Decay life time (ns)			Fractional contribution			X^2	Average lifetime (ns)
	τ_1	τ_2	τ_3	f_1	f_2	f_3		
CN	0.95	3.37	13.38	32.5	46.2	21.3	1.15	4.71
MC-6/CN	0.94	3.58	14.70	31.6	49.1	19.2	1.15	4.88
MC-9/CN	1.20	4.09	15.61	33.0	49.7	17.3	1.11	5.13
MC-12/CN	1.27	4.24	15.37	36.3	45.5	18.2	1.30	5.19
MC-15/CN	1.37	4.39	16.39	33.5	50.7	15.8	1.19	5.27
MC-18/CN	1.33	4.30	15.70	40.2	44.9	15.0	1.26	4.80

Table S4. The ΔG_{H*} values of all the adsorption models.

Models	Adsorption site (Model)	ΔG_{H*} (eV)
g-C_3N_4	C (S8.a)	-0.2301
	N (S8.b)	1.7146
α-MoC/g-C_3N_4	C_1 (S9.a)	-0.0443
	Mo_1 (S9.b)	-0.0751
	Mo_2 (S9.c)	-0.9347
	Mo_3 (S9.d)	-0.3280
	Mo_4 (S9.e)	0.3858

Supplementary References

1 H. Shi, Z. Sun, W. Lv, S. Wang, Y. Shi, Y. Zhang, S. Xiao, H. Yang, Q.-H. Yang and F. Li, Necklace-like MoC sulfiphilic sites embedded in interconnected carbon networks for Li–S batteries with high sulfur loading, *J. Mater. Chem. A.*, 2019, **7**, 11298-11304.

2 Y. Liu, X. Zhu, Q. Zhang, T. Tang, Y. Zhang, L. Gu, Y. Li, J. Bao, Z. Dai and J.-S. Hu, Engineering Mo/Mo_2C/MoC hetero-interfaces for enhanced electrocatalytic nitrogen reduction, *J. Mater. Chem. A.*, 2020, **8**, 8920-8926.

3 Z. Yan, G. He, P. K. Shen, Z. Luo, J. Xie and M. Chen, MoC-graphite composite as a Pt electrocatalyst support for highly active methanol oxidation and oxygen reduction reaction, *J. Mater. Chem. A.*, 2014, **2**, 4014.

4 M. Li, Y. Zhu, H. Wang, C. Wang, N. Pinna and X. Lu, Ni strongly coupled with Mo_2C encapsulated in nitrogen-doped carbon nanofibers as robust bifunctional catalyst for overall water splitting, *Adv. Energy Mater.*, 2019, **9**, 1803185.

5 Y. Y. Chen, Y. Zhang, W. J. Jiang, X. Zhang, Z. Dai, L. J. Wan and J. S. Hu, Pomegranate-like N,P-doped Mo_2C@C nanospheres as highly active electrocatalysts for alkaline hydrogen evolution, *ACS Nano*, 2016, **10**, 8851-8860.

6 H. Yan, Y. Xie, Y. Jiao, A. Wu, C. Tian, X. Zhang, L. Wang and H. Fu, Holey reduced graphene oxide coupled with an Mo_2N-Mo_2C heterojunction for efficient hydrogen evolution, *Adv. Mater.*, 2018, **30**, 1704156.

7 Y. Liu, Y. Zhang, Y. Zhang, Q. Zhang, X. Gao, X. Dou, H. Zhu, X. Yuan and L. Pan, MoC nanoparticle-embedded carbon nanofiber aerogels as flow-through

electrodes for highly efficient pseudocapacitive deionization, *J. Mater. Chem. A.*, 2020, **8**, 1443-1450.

8 J. Liu, P. Wang, J. Fan, H. Yu and J. Yu, Hetero-phase MoC-Mo_2C nanoparticles for enhanced photocatalytic H_2-production activity of TiO_2, *Nano Res.*, 2020, **14**, 1095-1102.

9 F. Yang, D. Liu, Y. Li, L. Cheng and J. Ye, Lithium incorporation assisted synthesis of ultra-small Mo_2C nanodots as efficient photocatalytic H_2 evolution cocatalysts, *Chem. Eng. J.*, 2020, **399**, 125794.

10 Y. Liu, G. Yu, G. D. Li, Y. Sun, T. Asefa, W. Chen and X. Zou, Coupling Mo_2C with nitrogen-rich nanocarbon leads to efficient hydrogen-evolution electrocatalytic sites, *Angew. Chem. Int. Ed.*, 2015, **54**, 10752-10757.

11 Y. Huang, Q. Gong, X. Song, K. Feng, K. Nie, F. Zhao, Y. Wang, M. Zeng, J. Zhong and Y. Li, Mo_2C nanoparticles dispersed on hierarchical carbon microflowers for efficient electrocatalytic hydrogen evolution, *ACS Nano*, 2016, **10**, 11337-11343.

12 X. Li, J. Zhang, R. Wang, H. Huang, C. Xie, Z. Li, J. Li and C. Niu, In situ synthesis of carbon nanotube hybrids with alternate MoC and MoS_2 to enhance the electrochemical activities of MoS_2, *Nano Lett.*, 2015, **15**, 5268-5272.

13 L. Lin, Q. Yu, M. Peng, A. Li, S. Yao, S. Tian, X. Liu, A. Li, Z. Jiang, R. Gao, X. Han, Y. W. Li, X. D. Wen, W. Zhou and D. Ma, Atomically dispersed Ni/alpha-MoC catalyst for hydrogen production from methanol/water, *J. Am. Chem. Soc.*, 2021, **143**, 309-317.

14 Y. Deng, R. Gao, L. Lin, T. Liu, X. D. Wen, S. Wang and D. Ma, Solvent tunes the selectivity of hydrogenation reaction over alpha-MoC catalyst, *J. Am. Chem. Soc.*, 2018, **140**, 14481-14489.

15 F. Gao, Y. Zhao, L. Zhang, B. Wang, Y. Wang, X. Huang, K. Wang, W. Feng and P. Liu, Well dispersed MoC quantum dots in ultrathin carbon films as efficient co-catalysts for photocatalytic H_2 evolution, *J. Mater. Chem. A.*, 2018, **6**, 18979-18986.

16 C. Wan, N. A. Knight and B. M. Leonard, Crystal structure and morphology control of molybdenum carbide nanomaterials synthesized from an amine-metal oxide composite, *Chem Commun (Camb)*, 2013, **49**, 10409-10411.

17 J. Dong, Y. Shi, C. Huang, Q. Wu, T. Zeng and W. Yao, A new and stable Mo-Mo_2C modified g-C_3N_4 photocatalyst for efficient visible light photocatalytic H_2 production, *Appl. Catal. B Environ.*, 2019, **243**, 27-35.

18 J. Zhang, M. Wu, B. He, R. Wang, H. Wang and Y. Gong, Facile synthesis of rod-like g-C_3N_4 by decorating Mo_2C co-catalyst for enhanced visible-light photocatalytic activity, *Appl. Surf. Sci.*, 2019, **470**, 565-572.

19 D. Zeng, P. Wu, W.-J. Ong, B. Tang, M. Wu, H. Zheng, Y. Chen and D.-L. Peng, Construction of network-like and flower-like 2H-$MoSe_2$ nanostructures coupled with porous g-C_3N_4 for noble-metal-free photocatalytic H_2 evolution under visible light, *Appl. Catal. B Environ.*, 2018, **233**, 26-34.

20 K. He, J. Xie, Z. Yang, R. Shen, Y. Fang, S. Ma, X. Chen and X. Li, Earth-abundant WC nanoparticles as an active noble-metal-free co-catalyst for the

highly boosted photocatalytic H_2 production over g-C_3N_4 nanosheets under visible light, *Catal. Sci. Technol.*, 2017, **7**, 1193-1202.

21 Y. Zhou, X. Ye and D. Lin, One-pot synthesis of non-noble metal WS_2/g-C_3N_4 photocatalysts with enhanced photocatalytic hydrogen production, *Int. J. Hydrogen Energy*, 2019, **44**, 14927-14937.

22 P. Ye, X. Liu, J. Iocozzia, Y. Yuan, L. Gu, G. Xu and Z. Lin, A highly stable non-noble metal Ni_2P co-catalyst for increased H_2 generation by g-C_3N_4 under visible light irradiation, *J. Mater. Chem. A.*, 2017, **5**, 8493-8498.

23 L. Ge and C. Han, Synthesis of MWNTs/g-C_3N_4 composite photocatalysts with efficient visible light photocatalytic hydrogen evolution activity, *Appl. Catal. B Environ.*, 2012, **117-118**, 268-274.